Rolling Bearing Calculations with Consideration of Geometric Deviations

Vincent Kramer, M. Sc.; Dr.-Ing. Marcel Bartz; Dr.-Ing. Stefan Götz; Prof. Dr.-Ing. Benjamin Schleich; and Prof. Dr.-Ing. Sandro Wartzack

Rolling bearing calculations are usually based on the assumption of ideal nominal geometries. However, actual components and assemblies are always subject to statically distributed geometric deviations resulting from the manufacturing and assembly processes. This leads to changes in the internal geometric conditions which have an effect on bearing characteristics such as the service life. The *FVA-Workbench* makes it possible for users to consider these geometric deviations in bearing calculations for more reliable results.

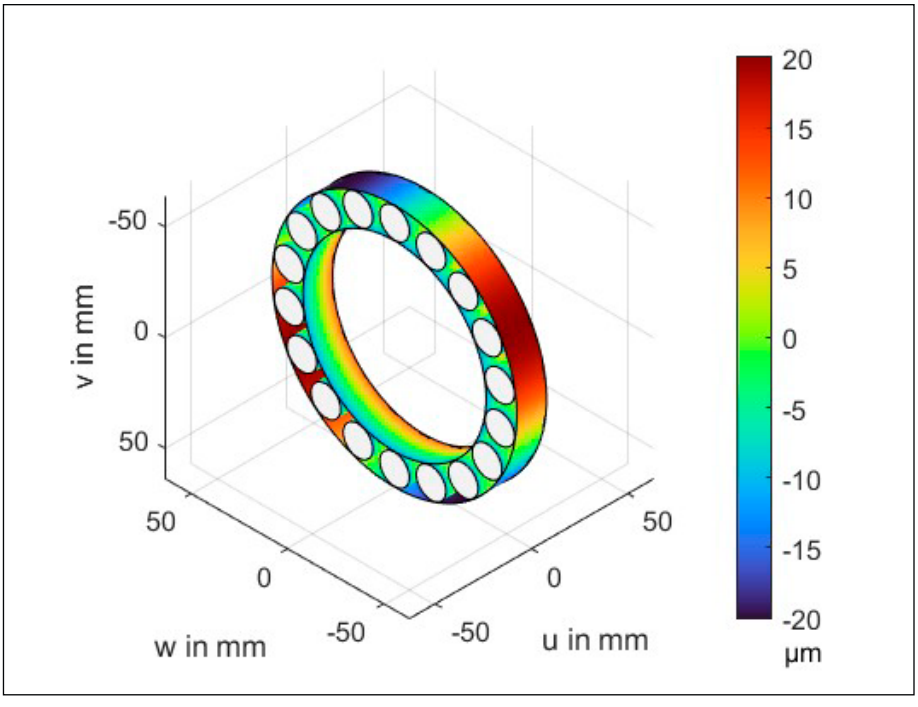

The raceways of a cylindrical roller bearing with a tapered geometric deviation of the inner ring raceway and ovalization of the outer ring raceway.

Problem Statement

Rolling bearings are indispensable components in all fields of mechanical engineering which allow for precise, low-friction, and cost-effective bearing arrangements for rotating components. Rolling bearings are typically calculated according to ISO/TS 16281. This generally assumes an ideal geometry for the actual raceways with no misalignment of the bearing axes.

However, this ideal situation can never be achieved in practice. The manufacturing and assembly processes always lead to geometric deviations which are expressed as a static distribution (Ref. 2). Furthermore, the loads during operation can cause deformations which influence the operating behavior of the bearings. For example, Fingerle (Ref. 3) has shown that meshing forces acting on the planetary gears cause ovalization of the wheel body. This leads to an increased or reduced bearing life compared to an ideally stiff wheel, depending on the conditions.

The integration of geometric deviations and their statically distributed characteristics in rolling bearing calculations results in a more accurate representation, which leads to improved results.

The *FVA-Workbench* (Ref. 4) software allows users to consider these form and position deviations in rolling bearing designs. The scripting interface also makes it possible to integrate user-defined routines. The following will show how these options can be used to perform bearing calculations, taking these statically distributed geometric deviations into consideration.

Consideration of Geometric Deviations in Rolling Bearing Design

The *FVA-Workbench* can be used for the modeling, configuration, and calculation of transmission systems. When modeling the entire system, an STP file of the casing can be imported, which can be then coupled with the bearing outer ring via a simple click workflow. This makes it possible to calculate the stiffness matrix and determine the equivalent stiffness according to Guyan (Ref. 5) without the use of external FE software. In addition to using bearing data according to manufacturer specifications (e.g., from rolling bearing catalogs), the rolling bearing geometry can also be directly specified. This includes profiling of the rolling elements and raceways, which makes it easy to consider form deviations.

Deviations on the outer ring raceway can be defined as radial deviations from the ideal circular form. For example, this can be used to define ovalization of the outer bearing ring.

Figure 1 shows an example of form deviation of the outer ring, enhanced one-hundred-fold for clarity.

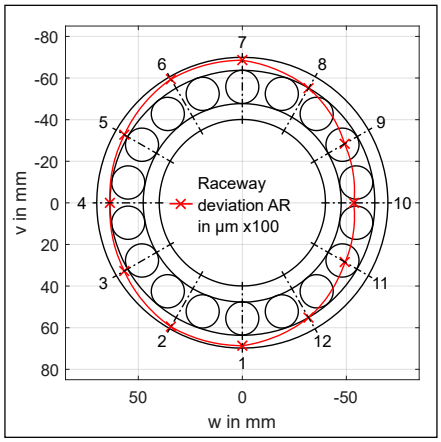

Figure 1—Example of form deviation of the outer ring raceway along the circumference (AR ≙ outer ring), illustration enhanced one-hundred-fold.

For rolling bearings with line contact, any kind of profiling can be defined in the axial direction for the rolling elements on the inner and outer ring.

Generally, manufacturers use specifically designed profile functions to improve the service life. In theory, however, any kind of form deviation of the raceways can be represented.

Figure 2 shows some example deviations in the axial direction with eight interpolation points. The rolling elements correspond to the suggested profile according to DIN 26281—with a crowned form deviation on the inner ring and a tapered form deviation on the outer ring. These values are also enhanced one-hundred-fold for clarity.

When using the slice model, DIN 26281 prescribes dividing the bearing into at least 30 axial slices. The *FVA-Workbench* supports any resolution, as long as this lower limit is not exceeded. For optimal resolution of the desired profiling in the slice model, a number of profiling interpolation points at least equal to the number of slices should be selected.

On the outer ring, additive deviations can be overlaid in both the longitudinal and circumferential directions.

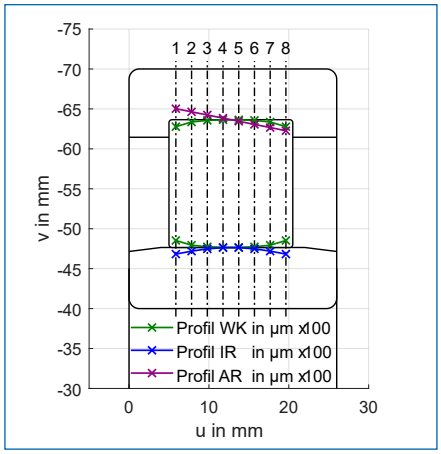

Figure 2—Example of form deviation in the axial direction (profilings) on a cylindrical roller bearing (WK ≙ rolling element, IR ≙ inner ring, AR ≙ outer ring), illustration enhanced one-hundred-fold.

In addition to these deviations on the raceways, an offset and misalignment of the casing-bearing seat can also be defined by specifying values for the vertical (v) and transverse (w) axes (for identification of the axes, see Figure 4). In the calculation, these values represent boundary conditions that are considered accordingly in solving the quasi-static equilibrium in the shaft-bearing-casing system.

The Scripting Module (Ref. 6) can be used to automate complex processes in the *FVA-Workbench*. Simple commands can be used to load additional data, run calculations, and create custom output reports. Possible output formats include simple text files, clearly prepared HTML reports or ready-configured *Excel* files.

For example, the Scripting Module can be used to load previously generated samples and process them in sequence. In this case, a sample describes a possible configuration of deviations as they can occur in reality.

Figure 3 shows the sequence for the statistical tolerance analysis in this example. The calculation is configured in an XML file in which the components and the form and position

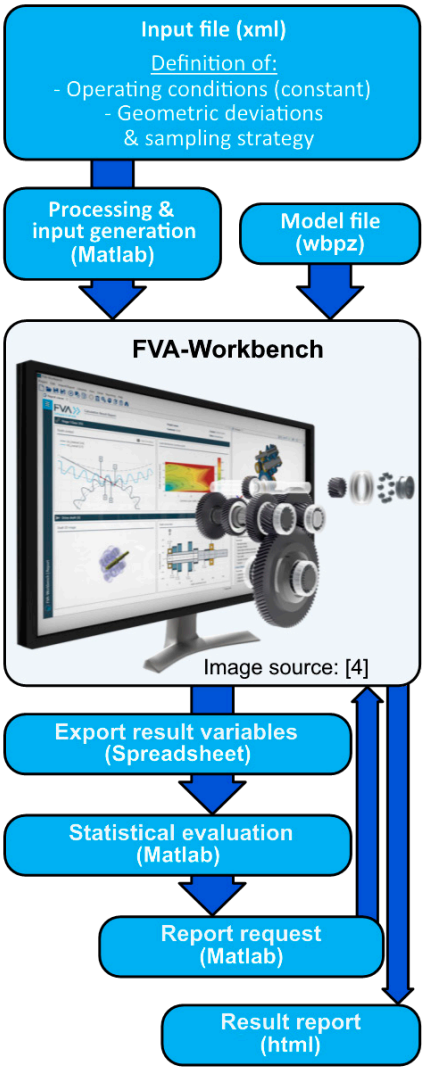

Figure 3—FVA-Workbench statistical tolerance analysis sequence for rolling bearing calculations.

deviations are defined. The samples are then automatically created based on the input file and the configured sampling strategy (randomly or systematically according to an experimental plan). The input file is processed by a MATLAB script, which saves the geometry data of the individual samples in an Excel file that can be read by the *FVA-Workbench*. A model file for which the calculations are to be performed is also required as an input.

The *FVA-Workbench* is then started in Batch Mode via a command line call and automatically processes the generated samples and saves the calculation results in an Excel file.

The statistical analysis of the results is then performed using suitable MATLAB scripts. A results report can also be generated for individual samples in the *FVA-Workbench*. This report is output in HTML format and includes detailed, graphical calculation reports for the individual system components (e.g., shaft bending, flank pressure in tooth meshes, or lifetime).

Parameter	Value	Unit
Casing material	EN-GJL-200	-
Shaft material	16MnCr5	-
Shaft diameter d	90	mm
Rotational speed	2000	1/min
Radial force F	66.4	kN
Relative bearing load C/P	5	-
Bearing distance	356	mm
Bearing I type (LI)	NU216	-
Bearing II type (LII)	NUP216	-
Bearing clearance class	CN	-
Rolling element profile	DIN 26281	-
Outer ring temperature	70	°C
Inner ring temperature	75	°C
Rolling element temperature	77	°C
Lubricant	FVA3	-
Lubricant temperature	47	°C

Table 1—Constant calculation parameters.

Calculation Example

The following example will demonstrate the sequence using a simple system consisting of a casing and shaft with a fixed-floating bearing arrangement with a radial force F acting on the center of the shaft (see Figure 4).

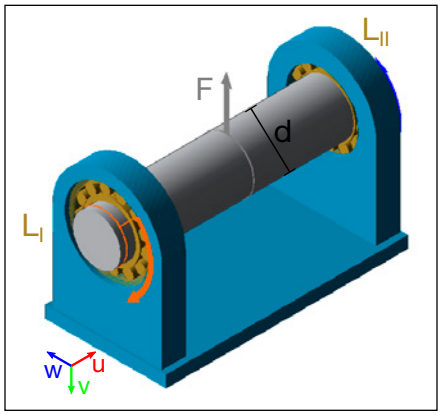

Figure 4—System model for the calculation.

Table 1 above provides an overview of the constant calculation parameters:

In addition to these constant parameters, a variable ovalization of the outer ring is also specified for Bearing I. The ovalization has an amplitude between 0 µm and 20 µm with a phase angle between 0 degrees and 360 degrees, modeled using a discrete Fourier transformation (DFT). Furthermore, a taper of the inner ring is also simulated with a value range of -5 to 5 angular minutes (').

The ovalization is represented in the *FVA-Workbench* as a form deviation of the outer ring in the circumferential direction (cf. Figure 1), whereas the taper is represented as an axial form deviation of the inner ring (cf. Figure 2). Furthermore, variation of the bearing clearance within the permissible limits of class CN is considered for both bearings. For bearing types NU216 and NUP216, this corresponds to an interval between 40 µm and 75 µm according to DIN 620-4 (Ref. 7). This is modeled as a change to the diameter of the outer ring, which is added to the ovalization.

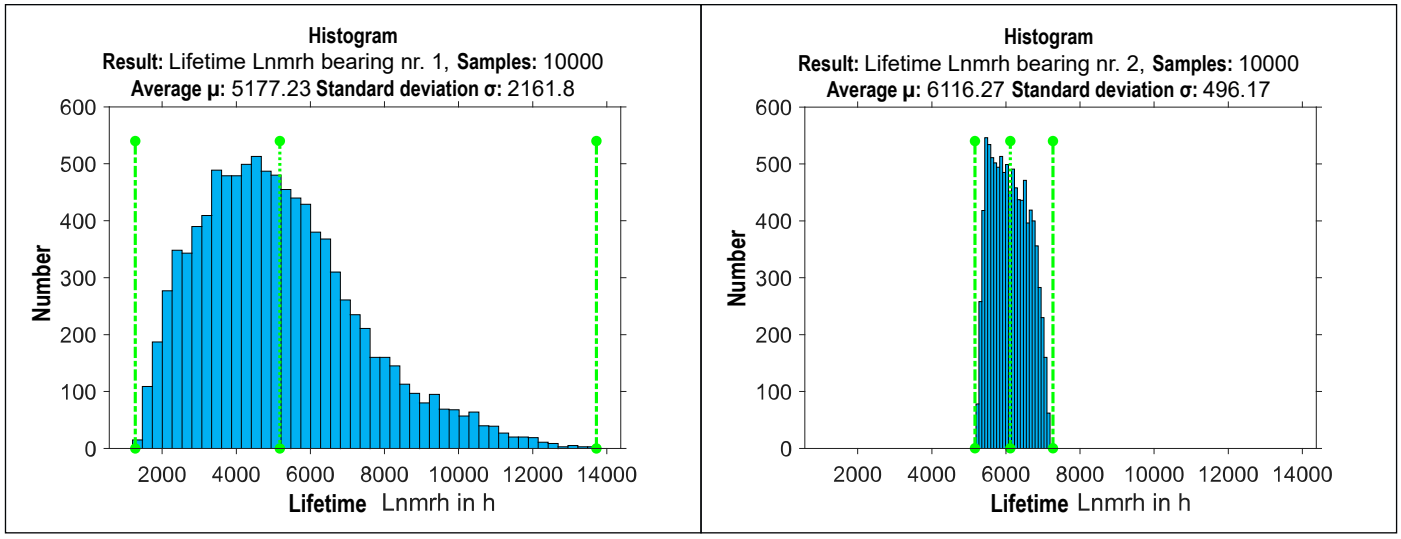

Figure 5—Lifetime L_{nmrh} histograms for Bearing I (left) and Bearing II (right).

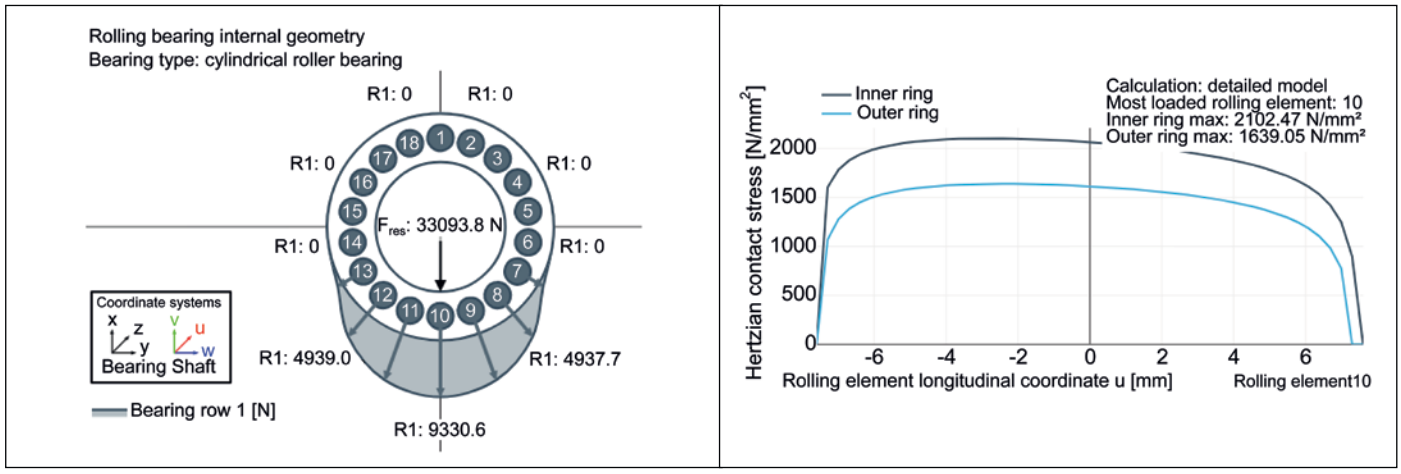

Figure 6—Rolling element load distribution (left) and axial pressure curve at the most heavily loaded rolling element (right) with median lifetime Lnmrh on Bearing II.

The concrete values for each individual sample are determined by Latin Hypercube Sampling.

A total of 10,000 individual cases are evaluated, with the sampling of the variable values following a Latin Hypercube Design (LHD) with minimized correlation of the variables. This sampling strategy achieves the best possible coverage of the space (Ref. 8). The calculation time is just under 90 minutes on a desktop workstation.

Figure 5 shows the distributions of the resultant modified reference lifetimes in hours (L_{nmrh}) according to DIN 26281 for both bearings in histogram form. It can be observed that the scatter is much greater for Bearing I than Bearing II. The value range for the lifetime of Bearing I extends beyond that of Bearing II on both sides, meaning that both higher and lower lifetimes can occur than with Bearing II. This is due to the defined geometric deviations on Bearing I, the effects of which will be analyzed in more detail below.

For reference, the internal bearing load distribution on the rolling elements, as well as the axial pressure curves of the most highly loaded rolling element (number 10) for the inner and outer ring contact from the *FVA-Workbench* report, are shown in Figure 6 for the median value (6096 h) of the lifetime L_{nmrh} on Bearing II (where only the bearing clearance is varied within the limits of class CN). The deflection and the pressure distribution of the bearings are calculated according to Teutsch & Sauer (Ref. 9). The rolling element load distribution (top) follows the typical arc-shaped curve, whereas the pressures in the axial direction (bottom) increase due to the shaft bending in the negative u-direction. It should be noted that greater Hertzian pressure occurs on the inner ring than on the outer ring due to the deforming contact.

By comparison, Figure 7 shows a visualization of the raceway geometries as well as the associated rolling element load distribution and axial pressure curves for the samples with minimum (left) and maximum (right) lifetime L_{nmrh} of Bearing I. As can be seen, there is clear ovalization of the outer ring raceway in both cases. For the sample with maximum

Min. lifetime Bearing I

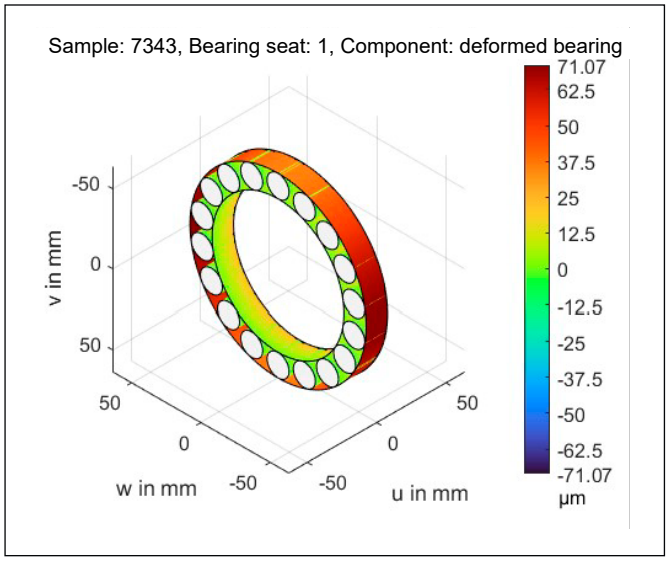

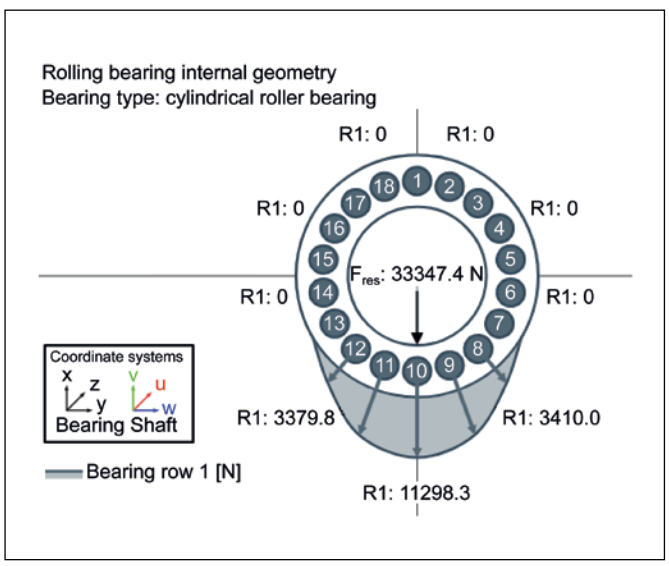

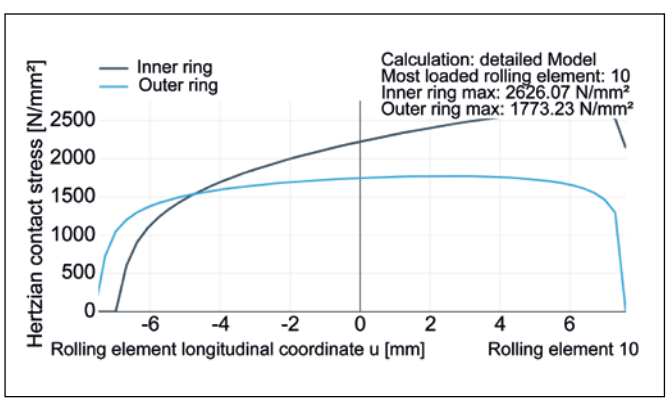

Max. lifetime Bearing

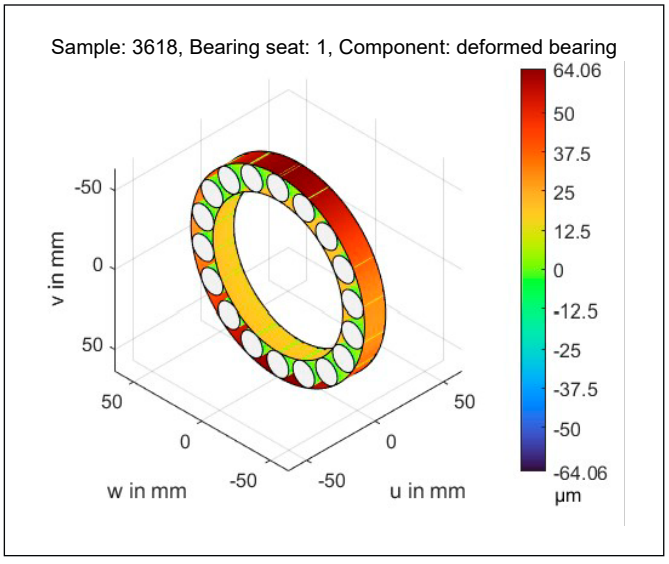

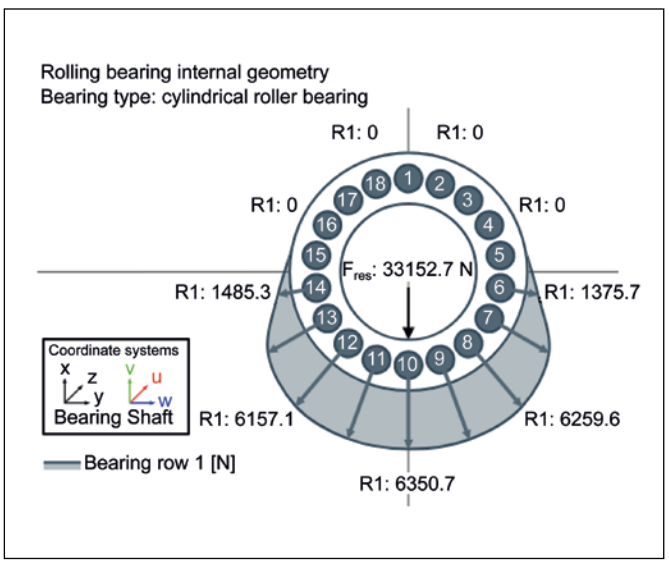

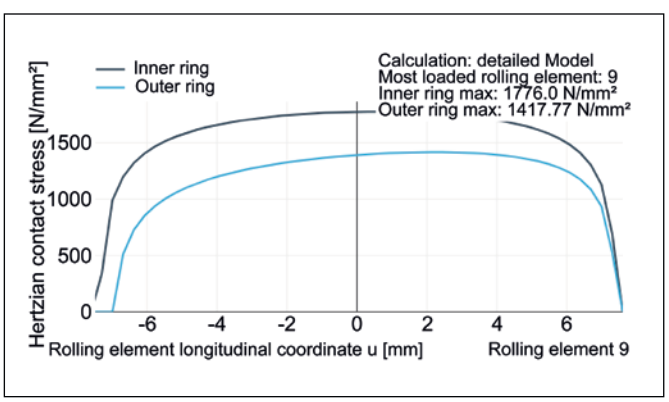

Figure 7—Raceway geometry (top), rolling element load distribution (middle), and axial pressure curve at the most heavily loaded rolling element (bottom) with minimum (left) and maximum (right) lifetime L_{amrh} on Bearing I.

lifetime, the value is 18.06 µm. The large semi-axis is aligned parallel to the load. In this case, the inner ring raceway shows a taper with a negative pitch in the u-direction. The associated lead angle is -0.98 angular minutes.

Here, the lifetime L_{nmrh} of 13721 h is more than double the mean value of 6096 h for Bearing II, which is due to the positive influence of the geometric deviations on the internal bearing load conditions. In comparison to Bearing II, the ovalization leads to a more uniform load distribution on the rolling elements, and thus a significant reduction in the peak load (compare Figure 6 top and Figure 7 middle-right). While the maximum rolling element load is 9330.60 N for Bearing II, in the best case it is only 6350.70 N for Bearing I.

The taper on the inner ring compensates for the bending of the shaft. As a result, the axial pressure curve of the inner ring is almost symmetrical to the center line. The maximum Hertzian pressure sinks to 1776.0 MPa compared to 2102.47 MPa for Bearing II (compare Figure 6 bottom and Figure 7 bottom-right). This is also a result of the reduced rolling element load.

On the other hand, the geometric deviations have the opposite effect for the sample with the minimum lifetime. In this case, the bearing lifetime is greatly reduced to 1273 h compared to the mean value of 6096 h for Bearing II. Here, too, the outer ring is ovalized. The amplitude of 18.08 µm is almost the same as in the optimum case. However, the large semi-axis is transverse to the load direction (compare Figure 7 top left and right). This results in a more uneven load distribution on the rolling elements, and thus an additional increase to the peak load on the most highly loaded rolling element compared to Bearing II (11298.30 N, see Figure 7 center-left, compared to 9330.60 N, see Figure 6 top).

The lead angle of the taper is clearly positive (4.94'), which reinforces the axial stress gradient from the bending of the shaft. Instead of uniform load distribution in the circumferential and longitudinal directions as in the optimum case, the higher rolling element peak loads and the axial stress gradient lead to a pronounced maximum local stress at the edge of the most heavily loaded rolling element (maximum Hertzian pressure of 2626.07 MPa, compared to 1776 MPa in the optimum case or the Bearing II median lifetime of 2102.47 MPa, see Figure 6 bottom and Figure 7 bottom). As a result, the expected bearing life decreases significantly.

Conclusion

The example presented in this article clearly shows that geometric deviations of the bearing raceways have a significant influence on the key characteristics of rolling bearings, such as the lifetime considered here. In practice, this can be a result of deformation of the bearing rings during mounting due to bearing seat geometries that are not ideally cylindrical, for example. The effect depends on the bearing type and size as well as the operating conditions. However, this is not necessarily negative, and can even be clearly positive. The *FVA-Workbench* allows users to directly consider geometric deviations in bearing design. The integrated scripting interface also makes it possible to integrate user-defined calculation routines (e.g., ring deformations determined from FE calculations or statistical tolerance analysis) with little effort.

PTE

References

1. DIN 26281: Rolling bearings—Methods for calculating the modified reference rating life for universally loaded bearings; Beuth Verlag, Berlin, 2010.
2. Schleich, B.; Skin Model Shapes: A New Paradigm for the Tolerance Analysis and the Geometrical Variations Modelling in Mechanical Engineering. Dissertation Friedrich-Alexander-Universität Erlangen-Nürnberg, 2017.
3. Fingerle, A.; Hochrein, J.; et al.; "Theoretical Study on the Influence of Planet Gear Rim Thickness and Bearing Clearance on Calculated Bearing Life.," Journal of Mechanical Design, Vol. 142, No. 3, 2020.
4. *FVA Workbench: https://www.fva-service.de/en/software/*
5. Guyan, R.; "Reduction of Stiffness and Mass Matrices," *AIAA Journal,* Vol. 3, No. 2, 1965.
6. FVA-Workbench Scripting Interface Documentation: *https://doc.fva-service.de/80/en/scripting.html*
7. DIN 620-4: Rolling bearings—Rolling bearing tolerances—Part 4: Radial internal clearance; Beuth Verlag, Berlin, 2004.
8. Siebertz, K.; van Bebber, D.; Hochkirchen, T.; Statistische Versuchsplanung, Design of Experiments (DoE), Springer Verlag, Berlin, Heidelberg, 2017.
9. Teutsch, R.; Sauer, B.; "An Alternative Slicing Technique to Consider Pressure Concentrations in Non-Hertzian Line Contacts," *Journal of Tribology,* Vol. 126, No. 3, 2004, pp. 436–442.